1998

The Role of Oxygen at the Second Discharge Plateau of Nickel Hydroxide

Sathya Motupally
University of South Carolina - Columbia

Mukul Jain
University of South Carolina - Columbia

Venkat Srinivasan
University of South Carolina - Columbia

John W. Weidner
University of South Carolina - Columbia, weidner@engr.sc.edu

Publication Info

Journal of the Electrochemical Society, 1998, pages 34-39.

τ dimensionless time, $(t\,|i|/nFc_{Ni}l)$
$\bar{\tau}$ dimensionless time at end of charge or discharge, $(\bar{t}\,|i|/nFc_{Ni}l)$

REFERENCES

1. K. Micka and I. Rousar, *Electrochim. Acta*, **25**, 1085 (1980).
2. K. Micka and I. Rousar, *ibid.*, **27**, 765 (1982).
3. J. Bouet, F. Richard, and P. Blanchard, in *Nickel Hydroxide Electrodes*, D. A. Corrigan and A. H. Zimmerman, Editors, PV 90-4, p. 260, The Electrochemical Society Proceedings Series, Pennington, NJ (1990).
4. D. Fan and R. E. White, *This Journal*, **138**, 17 (1991).
5. D. Fan and R. E. White, *ibid.*, **138**, 2952 (1991).
6. Z. Mao, P. De Vidts, R. E. White, and J. Newman, *ibid.*, **141**, 54 (1994).
7. J. W. Weidner and P. Timmerman, *ibid.*, **141**, 346 (1994).
8. P. De Vidts and R. E. White, *ibid.*, **142**, 1509 (1995).
9. B. V. Ratnakumar, P. Timmerman, C. Sanchez, S. Di Stefano, and G. Halpert, *ibid.*, **143**, 803 (1996).
10. B. Paxton and J. Newman, *ibid.*, **143**, 1287 (1996).
11. P. De Vidts, J. Delgado, and R. E. White, *ibid.*, **143**, 3223 (1996).
12. S. Motupally, C. C. Streinz, and J. W. Weidner, *ibid.*, **142**, 1401 (1995).
13. A. H. Zimmerman and P. K. Effa, Abstract 28, p. 43, The Electrochemical Society Meeting Abstracts, Las Vegas, NV, Oct. 13-18, 1985.
14. C. C. Streinz, A. P. Hartman, S. Motupally, and J. W. Weidner, *This Journal*, **142**, 1084 (1995).
15. C. C. Streinz, S. Motupally, and J. W. Weidner, *ibid.*, **142**, 4051 (1995).
16. D. M. MacArthur, *ibid.*, **117**, 442 (1970).
17. P. D. Lukovtsev and G. D. Slaidin, *Electrochim. Acta*, **6**, 17 (1962).
18. J. McBreen, in *Modern Aspects of Electrochemistry*, Vol. 21, R. E. White, J. O'M. Bockris, B. E. Conway, Editors, Plenum Press, New York (1990).
19. M. Jain, S. Motupally, and J. W. Weidner, in *Aqueous Batteries*, P. D. Bennett and S. Gross, Editors, PV 96-16, p. 121, The Electrochemical Society Proceedings Series, Pennington, NJ (1997).
20. J. Crank, *The Mathematics of Diffusion*, p. 61, Oxford University Press, Oxford (1994).
21. K. E. Brenan, S. L. Campbell, and L. R. Petzhold, *Numerical Solution of Initial Value Problems in Differential-Algebraic Equations*, North Holland, New York (1989).
22. G. W. D. Briggs and M. Fleischmann, *Trans. Faraday Soc.*, **69**, 2397 (1971).
23. D. M. MacArthur, *This Journal*, **117**, 729 (1970).

The Role of Oxygen at the Second Discharge Plateau of Nickel Hydroxide

Sathya Motupally,* Mukul Jain,* Venkat Srinivasan,* and John W. Weidner**

Center for Electrochemical Engineering, Department of Chemical Engineering, University of South Carolina, Columbia, South Carolina 29208, USA

ABSTRACT

It was shown that the appearance of a secondary discharge plateau approximately 400 mV below the primary plateau can result from the reduction of oxygen. During the galvanostatic discharge of planar nickel-hydroxide films at room temperature and in 3 weight percent KOH solutions, the second discharge plateau was observed only in the presence of dissolved oxygen in the electrolyte. When the solution was deoxygenated, no residual capacity could be extracted from the films even at low discharge rates or from overcharged films. In addition, the duration of the second plateau is inversely proportional to the square of the discharge current, which is indicative of a diffusion-controlled process. The nickel hydroxide active material, rather than the electrolyte, seems to be the primary reservoir for the oxygen that is reduced on the second plateau.

Introduction

Nickel hydroxide is the active material in the positive electrode of many rechargeable battery systems (e.g., nickel/cadmium, nickel/zinc, nickel/hydrogen, and nickel/metal hydride). The charge/discharge reaction for the active material can be represented as

$$NiOOH + H_2O + e^- \underset{\text{charge}}{\overset{\text{discharge}}{\rightleftharpoons}} Ni(OH)_2 + OH^- \qquad [1]$$

During the discharge of nickel hydroxide, two voltage plateaus have been reported.[1-16] The first (primary) discharge plateau seen at a potential of approximately 300 mV vs. the Ag/AgCl reference electrode, corresponds to the useful operating voltage of a nickel battery and is due to the reduction of nickel oxyhydroxide [NiOOH] to nickel hydroxide [$Ni(OH)_2$] via reaction 1. The second discharge plateau occurs approximately at 400 mV negative of the primary discharge plateau. This second discharge plateau is reported mostly for low rate discharges with a capacity of approximately 10 to 50% of that extracted on the first plateau.[5]

The explanations given in the literature regarding the second discharge plateau can be divided into three different groups. First, Barnard *et al.*,[5] Zimmerman and Effa,[8] Zimmerman,[9] and Klaptse *et al.*[12] hypothesize that the second discharge plateau is due to a change in the electronic behavior of the nickel hydroxide active material. According to these authors, the active material is a good electronic conductor in the charged state, but its conductivity steadily decreases on discharge due to the depletion of charge carriers. They state that the active material acts as a semiconductor after a significant depletion of charge carriers at the substrate/active material interface. The remaining active material cannot be discharged at the potential of the main plateau resulting in a loss in useful capacity. The discharge on the second plateau stops after all of the remaining active material becomes depleted of charge carriers. The second explanation for the second discharge plateau is that it results from the reduction of intrinsically less-active nickel oxides [e.g., $Ni_3O_2(OH)_4$ or $Ni_3O_4 \cdot xH_2O$] which are formed as intermediates during the discharge of NiOOH.[1-7] In an attempt to test this hypothesis, Barnard *et al.*[5] and Falk[6] investigated the discharged active material via x-ray diffraction. The authors were unable to detect any less-active nickel oxides formed during cycling. Recently, Sac-Epee *et al.*[7] investigated the second plateau in chemically and electrochemically

* Electrochemical Society Student Member.
** Electrochemical Society Active Member.

impregnated porous nickel electrodes. In their experiments, a second plateau was observed only in chemically impregnated electrodes devoid of cobalt additives. The electrodes that exhibited a second plateau were also the only ones to contain significant amounts of the γ-phase. Therefore, they concluded that the second plateau results from the direct reduction of γ-NiOOH to β-$Ni(OH)_2$.

These first two explanations for the second plateau represent an inefficient use of the active material since the capacity is transferred to a voltage that is too negative to be useful. A third explanation put forth by Falk,[6] Zedner,[10] and Foerster[11] does not involve the nickel hydroxide active material. Although no conclusive evidence was presented, the authors state that the charge extracted on the second discharge plateau is not due to the reduction of the nickel hydroxide active material, but rather it is due to the reduction of molecular oxygen according to

$$O_2 + 2H_2O + 4e^- \rightarrow 4\ OH^- \quad E^\circ = 0.204\ V\ (vs.\ Ag/AgCl) \quad [2]$$

Falk[6] and Zedner[10] found that the capacity of the second discharge plateau from a sealed nickel/cadmium cell was a strong function of the air pressure inside the cell. The second plateau is observed approximately 300 to 400 mV below the equilibrium potential of reaction 2 due to slow kinetics. The role of oxygen on the second plateau, however, has been discounted by a number of researchers. For example, Barnard *et al.*[5] discharged porous nickel electrodes and they saw a second plateau whether or not they sparged the electrolyte with nitrogen. They felt this evidence along with the black color of the active material (characteristic of NiOOH) precluded oxygen and suggested a semiconductor effect.

Due to the inevitable presence of oxygen during normal battery operation, it is important to understand the role oxygen plays in the observance of the second plateau. Although the second plateau has been linked experimentally to capacity transfer,[1-5,7-10] the mere observance of a second plateau is not proof of this phenomenon. Using only the second plateau to study capacity transfer could lead to erroneous conclusions. Therefore, the objective of this study is to investigate the role of oxygen at the second discharge plateau by performing galvanostatic discharges on planar nickel hydroxide films in the presence and absence of oxygen dissolved in the electrolyte.

Experimental

Thin films of nickel hydroxide were deposited electrochemically onto 0.2 cm^2 of gold sputtered onto a quartz crystal in a procedure described in detail elsewhere.[17,18] A glass cell contained the gold working electrode, a platinum gauze counter electrode and a Ag/AgCl reference electrode. An electrochemical quartz crystal microbalance (Elchema Model EQCM-501) was used to measure the mass of the deposited films, and a Pine bipotentiostat/galvanostat (Model AFRDE5) was used to control the deposition current. The films studied here were deposited at room temperature in a bath consisting of 1.8 M $Ni(NO_3)_2$, 0.175 M $Co(NO_3)_2$, and 0.075 M $NaNO_3$ in a solvent mixture of 50 volume percent (v/o) ethanol and 50 v/o water using a cathodic current density of 5 mA/cm^2. The deposition times for a 70 and 105 μg were 28.0 and 42.0 min, respectively. The corresponding film thicknesses were estimated by dividing the mass by the product of the active-material density and the cross-sectional area. Using a density of 3.5 g/cm^3 [20] and an area of 0.2 cm^2, the 70 and 105 μg films had thicknesses of approximately 1.0 and 1.5 μm, respectively. An elemental analysis performed on dissolved films, using an atomic absorption spectrophotometer, showed that the Ni:Co ratio in the active material was 88:12. [21]

Once a film of desired thickness was deposited, the nickel nitrate solution was removed from the cell, the cell and film were rinsed with deionized water, and 65 cm^3 of 3.0 weight percent (w/o) (i.e., 0.53 M) KOH solution (Mallinckrodt AR grade in 18 MΩ DI water) was transferred to the cell. The system used for charging and discharging the active material consists of an EG&G PAR 273 potentiostat/galvanostat combined with EG&G PAR M270 software on an IBM compatible personal computer.

As-deposited nickel hydroxide films [$Ni(OH)_2$] are light green in color and after the first charge are converted to nickel oxyhydroxide [NiOOH], which is black in color. On discharge, the active material retains the black color. The film converts from black to green only if it is left on open circuit in KOH solution for an extended period of time (approximately 3 to 4 h) or if it is discharged past the first plateau for approximately 1 h. In this paper, a freshly deposited green film is referred to as fresh nickel hydroxide, a discharged black film is referred to as black nickel hydroxide, and a conditioned film that has been converted from black to green is referred to as aged nickel hydroxide.

For data collected on black and aged nickel hydroxide, the films were conditioned by first charging galvanostatically to 0.5 V vs. Ag/AgCl. The charging currents for the 1.0 and 1.5 μm films were 90 and 135 μA/cm^2, rspectively, which correspond to a 1 h charge. The charged films were than cycled 20 times at 5 mV/s from 0.5 to 0.0 V and discharged galvanostatically at the corresponding currents given above to 0.0 V. Before and between experiments on black films, 1 h charge was followed by two cycles at 5 mV/s from 0.5 to 0.0 V. For data collected on aged and fresh nickel hydroxide, the films remained in the discharged state until all data were collected.

For discharges performed in the absence of oxygen, the electrolyte was sparged with helium for approximately 40 min before the experiment and the sparging continued during the experiment. To saturate the electrolyte with oxygen, the gas was bubbled for approximately 20 min. To investigate the effect of the oxygen produced on overcharge, the glass cell was sealed after the electrolyte was deoxygenated. A Teflon® cap containing ports to accommodate the reference, the counter electrodes, and a sparging tube was used to seal the cell. A 1.5 μm nickel hydroxide film was used for the overcharge experiments (Fig. 2 and 3), whereas 1.0 μm films were used for all other experiments (Fig. 1, 4-8).

To measure the kinetic parameters for oxygen reduction, a constant cathodic current from 0.5 to 250 μA/cm^2 was applied while sparging the electrolyte with oxygen. A steady-state potential was reached in less than 1 min. After a set of current/voltage data was collected, a high frequency (100 kHz to 10 Hz) electrochemical impedance experiment (EIS) was conducted to adjust for uncompensated resistance. The measured voltages were reproducible to within 5%.

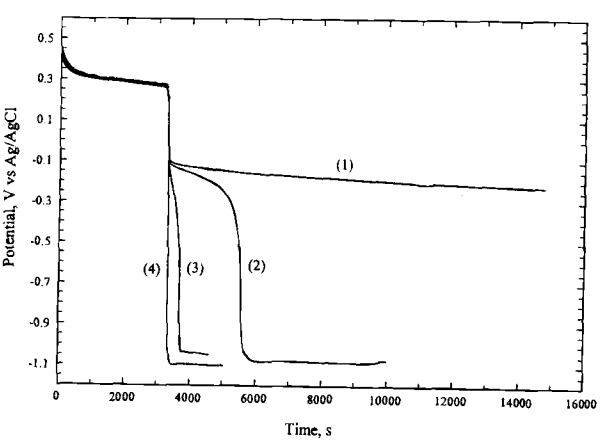

Fig. 1. Discharge curves obtained when the electrolyte was sparged with: (1) oxygen before and during the experiment; (2) oxygen before the experiment (3) neither helium nor oxygen; and (4) helium before and during the experiment. The discharge current density was 100 μA/cm^2 and the electrolyte was 3% KOH.

Results and Discussion

The effect of oxygen on the second discharge plateau is shown in Fig. 1. For the four curves, the electrolyte was sparged with: (1) oxygen before and during the experiment; (2) oxygen before the experiment (3) neither helium nor oxygen; (4) helium before and during the experiment. The first discharge plateau is similar in all four experiments and is due to the reduction of NiOOH to $Ni(OH)_2$ according to reaction 1. All discharges were performed at 100 $\mu A/cm^2$ with the first plateau lasting for approximately 3300 s, irrespective of the presence of oxygen. The charge extracted on the second discharge plateau decreases from an indefinite value for curve 1 to zero for curve 4. For conditions of curve 1, charge could be extracted on the second plateau for as long as the supply of oxygen was maintained. In one experiment, the second plateau was seen for as long as 72 h.

For discharge curve 2, the electrolyte was saturated with oxygen prior to the experiment with no stirring during the experiment. The result is a second plateau that continues for 2200 s. Curve 3 is a discharge in a freshly mixed electrolyte. In this case, oxygen dissolves from the atmosphere during the preparation of the electrolyte and results in a second plateau that lasts 200 s. Curve 4 is a discharge performed in an oxygen-free electrolyte. No measurable charge could be extracted on the second plateau even when the discharge current was decreased by a factor of 10. The third discharge plateau at approximately −1.0 V vs. Ag/AgCl is due to the reduction of water.

From the evidence in Fig. 1, the logical explanation for these second discharge plateaus is the reduction of oxygen via reaction 2. To show that the second plateau could also result from oxygen produced during overcharge, four different experiments were performed in a sealed cell. Prior to an experiment, helium gas was bubbled through the electrolyte to displace any existing oxygen. The cell was then sealed thus ensuring that the only oxygen in the electrolyte was that produced during overcharge. A 1.5 μm film was charged and discharged at a current density of 1.0 mA/cm^2 and 100 $\mu A/cm^2$, respectively. The only variable in the experiments was the duration of charge prior to discharge. The points A, B, C, and D in Fig. 2 correspond to 600, 3000, 6000, and 9000 s of total charging time, respectively. Point A represents the time required for the active material to be completely charged and further charging results in the oxidation of the electrolyte to produce oxygen.

The discharge curves corresponding to points A through D are shown in Fig. 3. The first plateau is unaffected by overcharge, but the duration of the second plateau increases with increasing degree of overcharge. Charging the electrode for 600 s (point A) produces a negligible amount of oxygen, and a second plateau is not seen on the corresponding discharge curve. However, overcharging the film to points B, C, and D results in the evolution of oxygen and the amount of oxygen produced increases with the increase in the duration of overcharge. As a result, the charge extracted on the second plateau increases with an increase in the duration of overcharge. The durations of the second plateau for discharge curves B, C, and D are approximately 860, 1700, and 2600 s, respectively. Repeating discharge curve D followed by 40 min of sparging with helium resulted in a discharge curve similar to curve A (i.e., no charge could be extracted at the potential of the second plateau). This latter result indicates that overcharge need not result in the formation of higher valent nickel compounds which are less active and discharge at the second plateau.

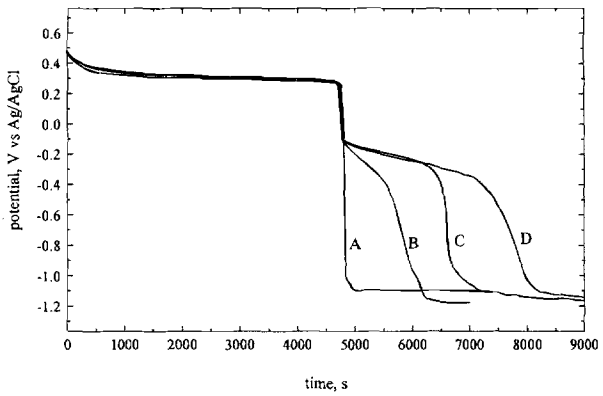

Fig. 3. Discharge curves as a function of degree of overcharge. The labels A-D correspond to the degree of overcharge as shown on the charge curve in Fig. 2. The discharge current was 100 $\mu A/cm^2$.

The association of the second plateau with the presence of oxygen is evident from Fig. 1-3. However, only a small fraction of the available oxygen is being reduced on the second plateau. For example, the solubility of oxygen in 3 w/o KOH is approximately 1.2 m*M*.[22] In order to consume all of the oxygen in 65 cm^3 of electrolyte, the second plateau in curve 2 of Fig. 1 would continue for over 400 h. Since the second plateau lasts only for 2200 s, less than 0.2% of the available oxygen is reacting on the second plateau. Similarly when comparing Fig. 2 and 3, only 3% of the coulombs delivered during overcharge are observed on the second discharge plateau (note that the charge current is ten times greater than the discharge current).

To determine if this low oxygen utilization is due to diffusion limitations of oxygen from the bulk electrolyte to the film surface, or if it is due to limited adsorption capac-

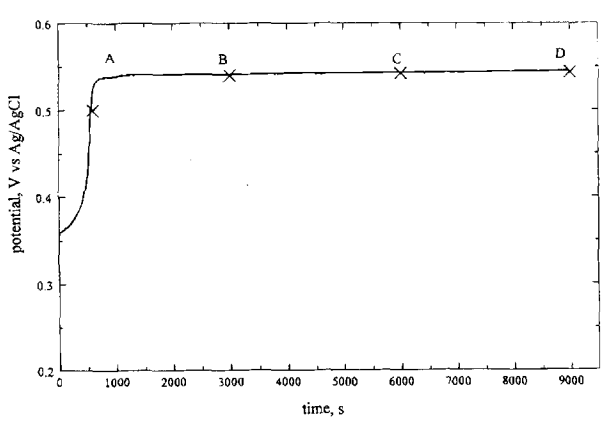

Fig. 2. A single charge curve for nickel hydroxide film showing different degrees of overcharge. The labels A-D indicate the times at which the charge was terminated for the discharge curves shown in Fig. 3. The charge current as 1 mA/cm^2.

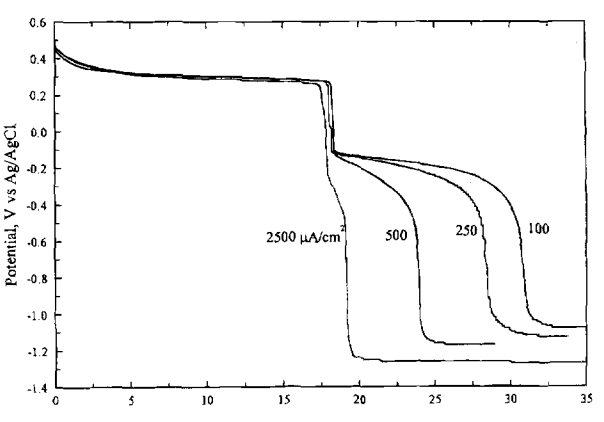

Fig. 4. Discharge curves as a function of applied current density. The charge extracted on the second plateau decreases with an increase in the applied current density.

ity of oxygen on the film, discharges were performed over a range of currents. Figure 4 is a plot of discharge voltage vs. capacity at four different discharge currents. The utilization of the primary discharge plateau decreases slightly with an increase in the applied current due to the diffusional limitations of protons in the nickel hydroxide film.[23] The capacity extracted on the second plateau also decreases but to a much larger extent. For example, as the current increases from 100 to 2500 $\mu A/cm^2$ the duration of the second discharge plateau decreases from 2200 to 6 s which corresponds to a decrease in capacity from 12.2 to 0.8 μAh.

If reaction 2 is diffusion limited, the length of the second plateau, τ, should be inversely proportional to the square of the discharge current as given by the Sand equation[24]

$$\sqrt{\tau} = \frac{nFC^{\circ}\sqrt{\pi D}}{2i} \quad [3]$$

where n is the number of electrons transferred per mole of reactant, F is Faraday's constant, D is the diffusion coefficient of the reactant, C° is the bulk concentration of oxygen, and i is the applied current density. Conversely, if the second discharge plateau is due to the reduction of adsorbed oxygen on the film, then the duration of the second plateau should be governed by Faraday's law, and τ will be given by

$$\tau = \frac{nFC^{*}}{i} \quad [4]$$

where C* the adsorbed oxygen concentration per unit area. Figure 5 is a plot of $\sqrt{\tau}$ vs. $1/i$ for current densities ranging from 150 to 2500 $\mu A/cm^2$ for a black nickel hydroxide film, whereas the inset shows a plot of τ vs. $1/i$ for the same data. The relatively straight line for $\sqrt{\tau}$ vs. $1/i$ as compared to the plot of τ vs. $1/i$ in the inset indicates that the second plateau is limited by the diffusion of oxygen to the surface of the electrode.

Although the linearity in the data for $\sqrt{\tau}$ vs. $1/i$ is not surprising, the resulting slope of the line is larger than expected. According to the Sand equation (Eq. 3), the slope of the line in Fig. 5 is $nFC^{\circ}\sqrt{\pi D}/2$. Assuming $D = 1.8 \times 10^{-5}\ cm^2/s$ [22] and $C^{\circ} = 1.2\ mM$ in 3 w/o KOH,[22] a slope of 0.0017 $s^{1/2}\ A/cm^2$ should be obtained. The slope of the linear fit of the data shown in Fig. 5 is 0.0053 $s^{1/2}\ A/cm^2$, a factor of three greater than that predicted by a process controlled by diffusion of oxygen from the bulk electrolyte to the surface.

To determine the reason for the large slope seen in Fig. 5, a series of galvanostatic discharges were performed on: (*i*) a bare gold substrate; (*ii*) a freshly deposited nickel hydroxide film; and (*iii*) an aged nickel hydroxide film. Figure 6 shows the $\sqrt{\tau}$ vs. $1/i$ data with the corresponding linear least-squares fit for the above-mentioned three cases and also for the black nickel hydroxide film from Fig. 5. The duration of the second plateaus reported in Fig. 5 and 6 (i.e., τ) is an average of three sets of data. The slope of the straight line for the bare gold electrode is 0.0021 $s^{1/2}\ A/cm^2$, a value that is 24% larger than the theoretical slope calculated above. This discrepancy is not unreasonable considering that the slope depends on the values used for the cutoff voltage, the oxygen concentration, and the diffusion coefficient. However, the experimental error caused by these factors will be the same for all four cases. Therefore, the large slopes derived from the data collected on the nickel hydroxide films cannot be explained by experimental error alone. It is also unlikely that the extra capacity measured in the presence of the film is due to the reduction of the less active material since the data collected on the green and black films produced comparable slopes. This refutes the theory that the conversion of the active material from black to green on the second discharge plateau is proof that the second plateau results from the reduction of less active nickel sites.[5]

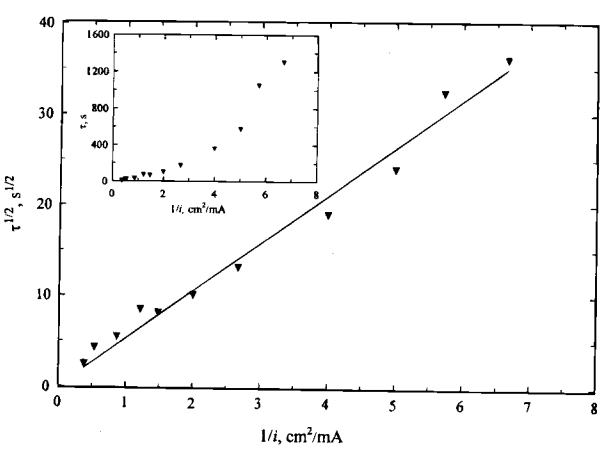

Fig. 5. Duration of the second discharge plateau, τ, as function of the applied current density, i, for a black nickel hydroxide film. The main plot shows data plotted as $\sqrt{\tau}$ vs. $1/i$ (see Eq. 3) and the inset shows the plot for τ vs. $1/i$ (see Eq. 4). The linearity of $\sqrt{\tau}$ vs. $1/i$ indicates that the process is primarily diffusion limited.

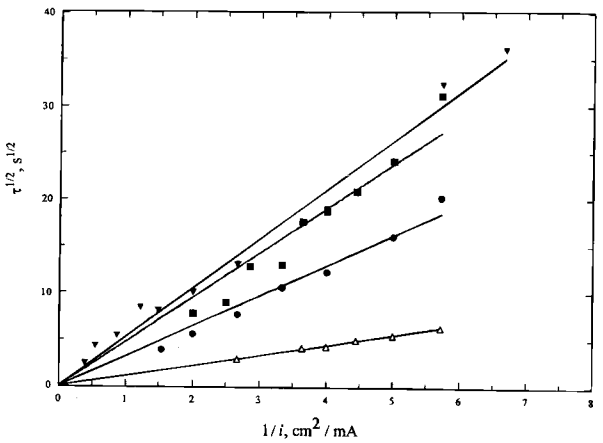

Fig. 6. Square root of the duration of the second discharge plateau, $\sqrt{\tau}$, as a function of the reciprocal of the applied current density, $1/i$, for: a bare gold electrode (Δ); a fresh nickel hydroxide film (●); and aged nickel hydroxide film (■); and a black nickel hydroxide film (▼). The data is plotted according to Eq. 3.

If a nondiffusional process (e.g., capacitive charging, discharge of less active nickel sites, reduction of adsorbed oxygen) is the source of the extra capacity, then the total current is the sum of the currents from the diffusional and nondiffusional processes. If these two parallel processes are relatively constant for the duration of the second plateau, then Eq. 3 and 4 can be rearranged and summed to give

$$i\tau = \frac{nFC^{\circ}\sqrt{\pi D}}{2}\sqrt{\tau} + nFC^{*} \quad [5]$$

Figure 7 is the data from the black film and bare gold electrode replotted as τ vs. $\sqrt{\tau}$. The slopes of the lines in Fig. 7 are identical to the ones found in Fig. 6 and they are a measure of the diffusional process. The intercepts are a measure of the charge extracted from a nondiffusional process. Although the intercept in Eq. 5 was derived for oxygen adsorption, it can also represent the charging of a capacitor or the reduction of residual nickel in the film. Intercepts of 0.003 C/cm^2 and 0.0 C/cm^2 were obtained for the black film and gold electrode, respectively. The intercept from the data on the black film corresponds to a duration of 30 s on the second plateau for the discharge current of 100 $\mu A/cm^2$. This is negligible compared to the total duration of the second discharge plateau (approximately 2200 s). Therefore, the duration of the second dis-

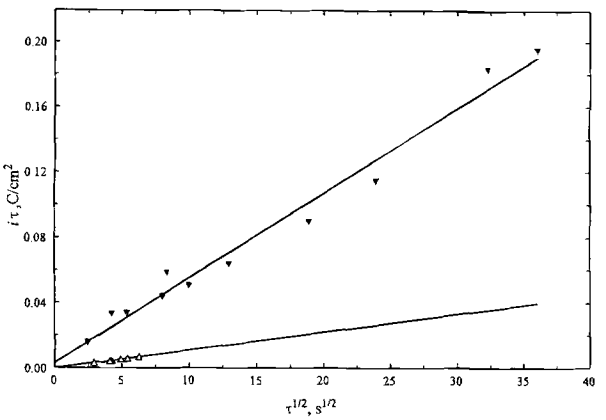

Fig. 7. Product of the applied current density and square root of the duration of the second discharged plateau, $i\sqrt{\tau}$ vs. the square root of the duration of the second discharge plateau, $\sqrt{\tau}$, for bare gold electrode (△), and the black nickel hydroxide film (▼).

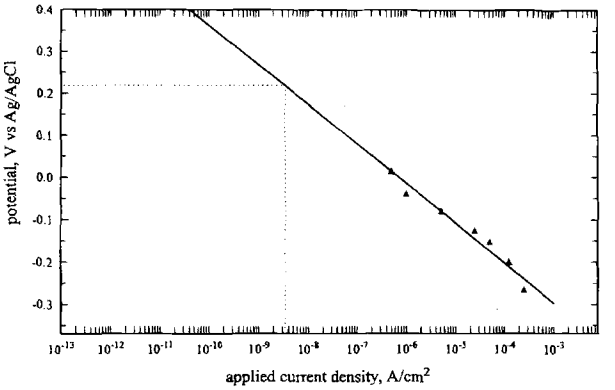

Fig. 8. Tafel plot for the oxygen reduction reaction. The exchange current density and the Tafel slope resulting from a least squares fit of the data are 3.0×10^{-9} A/cm^2 and 39 mV/decade, respectively.

charge plateau is governed primarily by diffusion of the reacting species.

The only other explanation for the slope being greater than the theoretical value in the presence of a film is that oxygen is absorbed in the film rather than adsorbed on the surface. However, the data will show only signs of diffusion control if the thickness of the diffusion layer, δ, is less than the thickness of the film, l, at the lowest applied current, and hence the longest duration of the second plateau. This inequality (i.e., $\delta \leq l = 1.0$ μm) can be used to estimate the upper limit of the diffusion coefficient for oxygen in the film. The slope in Fig. 6 can then be used to estimate the lower limit for the concentration of oxygen in the active material.

The diffusion layer thickness can be approximated by

$$\delta \approx \sqrt{D\tau} \qquad [6]$$

Setting $\delta = l = 1.0$ μm and $\tau = 1000$ s (at $i = 150$ μA/cm^2), the upper limit for D can be approximated from Eq. 6 to be on the order of 10^{-11} cm^2/s. Since this value of D is approximately six orders of magnitude smaller than the diffusion coefficient of oxygen in the electrolyte (10^{-11} cm^2/s vs. 10^{-5} cm^2/s), three orders of magnitude decreases in the slope should result. Therefore, to offset this decrease, the concentration of oxygen in the film must be three orders of magnitude greater than the corresponding concentration in the electrolyte (1 M vs. 1 m*M*) just to maintain a second plateau of duration equal to that on gold. To exceed the slope, the oxygen concentration in the film must be greater than 1 M.

An oxygen concentration in excess of 1 M is surprisingly large, but not impossible. One way to judge whether or not this value is realistic is to compare it to the concentration of nickel sites in the film. The nickel concentration can be calculated by dividing the density of the active material (3.5 g/cm^3 [20]) by its molecular weight (107 g/mol [18]) to give 0.033 mol/cm^3 or 33 M. Compared to this value, having one oxygen molecule for every 10 to 20 nickel sites is not unreasonable. Therefore, it is reasonable to assume that the active material can serve as a large reservoir for oxygen during reduction at the second plateau. This finding suggests that the studies on the second plateau in porous electrodes can lead to erroneous conclusions regarding the role of oxygen. For example, purging the electrolyte with an inert gas may take an excessively long period of time to eliminate all the oxygen from the active material. The high concentration and the low diffusion coefficient for oxygen in the film is also consistent with the finding that the second plateau is observed only at low discharge rates.[5] The active material serves as a significant barrier for oxygen diffusion which is amplified at high discharge rates.

It may be necessary to include oxygen reduction at the voltage of the second plateau in order to track oxygen when mathematically simulating sealed cells (see for example De Vidts *et al.*[15] Therefore, the kinetic parameters for oxygen reduction were measured from polarization data taken on black nickel hydroxide films. To eliminate mass-transfer effects, oxygen was bubbled through the solution during the experiment. The applied current densities ranged from 0.5 to 250 μA/cm^2, and the steady-state potential was compensated for the ohmic resistance. Figure 8 is a semilog plot of the applied current density vs. the potential (vs. Ag/AgCl). The Tafel slope measured from Fig. 8 is approximately 39 mV/decade. The theoretical equilibrium potential for oxygen evolution, under the experimental conditions of this study (i.e., partial pressure of oxygen of 1 atm and 3% KOH as electrolyte), is 0.218 V vs. the Ag/AgCl reference. The exchange current density of the oxygen reduction reaction, obtained from the intercept on the x-axis at the equilibrium potential value, is 3.0×10^{-9} A/cm^2.

Conclusions

The relationship between the second discharge plateau observed during the discharge of nickel hydroxide films and the presence of oxygen was investigated. It was found that the second discharge plateau was due to the reduction of oxygen. The second plateau was never observed in a deoxygenated electrolyte, but was always observed when oxygen was present in the electrolyte. In addition, the duration of the second plateau was inversely proportional to the square of the discharge current density, which is indicative of a diffusion-controlled process. By comparing discharge data collected on a gold electrode with and without nickel hydroxide films, it was concluded that oxygen in the active material contributes significantly to the supply of oxygen involved in the reduction reaction. Finally, the kinetic parameters for the reduction of oxygen were measured from polarization data.

Acknowledgments

The authors gratefully acknowledge the financial support from the Department of Energy by Cooperative Agreement DE-FCO2-91ER75666, Amendment No. A004.

Manuscript submitted Feb. 20, 1997; revised manuscript received July 18, 1997.

The University of South Carolina assisted in meeting the publication costs of this article.

REFERENCES

1. S. E. S. El Wakkard and E. S. Emara, *J. Chem. Soc.*, **4**, 35045 (1953).
2. J. Besson, *Ann. Chim.*, **2**, 527 (1947).
3. A. P. Rollet, *ibid.*, **13**, 217 (1930).
4. O. Glemser and J. Einerhand, *Z. Elektrochem.*, **54**, 302 (1950).

5. R. Barnard, G. T. Crickmore, J. A. Lee, and F. L. Tye, *J. Appl. Electrochem.*, **10,** 61 (1980).
6. S. U. Falk, *This Journal*, **8,** 659 (1960).
7. N. Sac-Epee, B. Beaudoin, A. Delahaye-Vidal, J-M. Tarascon, and T. Jamin, Abstract 881, p. 1086, The Electrochemical Society Meeting, Abstracts, Vol. 96-2, San Antonio, TX, Oct. 6-11, 1996.
8. A. H. Zimmerman and P. K. Effa, *This Journal*, **129,** 983 (1984).
9. A. H. Zimmerman in *Hydrogen and Metal Hydride Batteries*, P. D. Bennett and T. Sakai, Editors, PV 94-27, p. 268, The Electrochemical Society Proceedings Series, Pennington, NJ (1994).
10. J. Zedner, *Z. Elektrochem.*, **12,** 463 (1906).
11. F. Foerster, *ibid.*, **13,** 414 (1907).
12. B. Klaptse, J. Mrha, K. Micka, J. Jindra, and V. Marecek, *J. Power Sources*, **4,** 349 (1979).
13. P. C. Milner and U. B. Thomas, in *Advances in Electrochemistry and Electrochemical Engineering*, Vol. 5, C. W. Tobias, Editor, Interscience Publishers, New York (1967).
14. Z. Mao, P. De Vidts, R. E. White, and J. Newman, *This Journal*, **141,** 54 (1994).
15. P. De Vidts, J. Delgado, and R. E. White, *ibid.*, **143,** 3223 (1996).
16. J. McBreen, in *Modern Aspects of Electrochemistry*, Vol. 21, R. E. White, J. O'M. Bockris, and B. E. Conway, Editors, Plenum Press, New York (1990).
17. C. C. Streinz, A. P. Hartman, S. Motupally, and J. W. Weidner, *This Journal*, **142,** 1084 (1995).
18. C. C. Streinz, S. Motupally, and J. W. Weidner, *ibid.*, **142,** 4051 (1995).
19. B. A. Johnson, R. E. Ferro, G. M. Swain, and B. J. Tatarchuk, *J. Power Sources*, **47,** 251 (1994).
20. A. H. Zimmerman and P. K. Effa, Abstract 28, p. 43, The Electrochemical Society Meeting Abstracts, Vol. 85-2, Las Vegas, NV, Oct. 13-18, 1985.
21. S. Motupally, C. C. Streinz, and J. W. Weidner, *This Journal*, **142,** 1401 (1995).
22. K. E. Gubbins and R. D. Walker Jr., *ibid.*, **112,** 469 (1965).
23. S. Motupally, C. C. Streinz, and J. W. Weidner, *ibid.*, **145,** 29 (1998).
24. A. J. Bard and L. R. Faulkner, *Electrochemical Methods: Fundamentals and Applications*, p. 253, John Wiley & Sons, New York (1980).

The Role of Carbon Dioxide in the Atmospheric Corrosion of Zinc

A Laboratory Study

T. Falk, J.-E. Svensson and L.-G. Johansson*

Department of Inorganic Chemistry, Chalmers University of Technology and University of Göteborg, S-412 96 Göteborg, Sweden

ABSTRACT

We report on a laboratory study of the atmospheric corrosion of zinc in air containing different concentrations of carbon dioxide (CO_2) (<1, 350, 1000, and 40,000 ppm CO_2). The samples were exposed to synthetic atmospheres with careful control of CO_2 concentration, sulfur dioxide (SO_2) concentration, relative humidity, and flow conditions. The relative humidity was 95%. Mass gain and metal loss results are reported. The corrosion products were analyzed quantitatively and qualitatively by a combination of grazing-angle x-ray diffraction, scanning electron microscopy, gravimetry, and quantitative analysis for carbonate. The corrosion rate of zinc increased with increasing CO_2 concentration. In the presence of carbon dioxide $Zn_4CO_3(OH)_6 \cdot H_2O$ formed. Hydrozincite, $Zn_5(CO_3)_2(OH)_6$ was only identified after exposure to high CO_2 concentration. Zinc hydroxycarbonate was converted into hydroxysulfate exposed to air containing 225 ppb SO_2. $Zn_4SO_4(OH)_6 \cdot 4H_2O$ was produced in all exposures including SO_2. The zinc hydroxycarbonate surface film formed in the presence of CO_2 was not protective in humid SO_2 polluted air.

Introduction

The atmospheric corrosion of zinc is known to be influenced by a number of factors, including relative humidity, the frequency and pH of rain, and the presence of various pollutants.[1] The corrosivity of sulfur dioxide (SO_2) toward zinc has been demonstrated in several field studies and laboratory investigations.[2-13] The effect of other gaseous pollutants is less studied. However, laboratory investigations have demonstrated that ozone (O_3) and nitrogen dioxide (NO_2) strongly accelerate the atmospheric corrosion of zinc in the presence of SO_2.[12-15]

Hydroxycarbonates are frequently detected in the corrosion products formed on zinc in environments with low SO_2 levels.[3,16-22] There are few reports in the literature on the actual phase composition of carbonate containing zinc corrosion products. According to Feitknecht,[23] hydrozincite ($Zn_5(CO_3)_2(OH)_6$) is the thermodynamically most stable zinc corrosion product in unpolluted air, while other hydroxycarbonates that are closely related to hydrozincite also form, depending on conditions. The frequent occurrence of hydroxycarbonate corrosion products indicates that carbon dioxide (CO_2) plays an important role in the atmospheric corrosion of zinc.

Several authors[23,24] have suggested that the layer of zinc hydroxycarbonate formed on zinc in pure air has protective properties. Recently Odnevall *et al.*[19] suggested that hydroxy carbonates formed early during exposure are important intermediates in the subsequent formation of other corrosion products. However, in spite of the obvious importance of CO_2 in the atmospheric corrosion of zinc there are no laboratory studies addressing the role of CO_2.

The aim of this work is to study the influence of CO_2 on the corrosion of zinc in humid air and to investigate the corrosion products formed and their protective properties.

Experimental

Zinc of electrolytic grade (>99.9% purity) was used in all experiments. The zinc samples had a geometrical area of 20 cm^2 (3.0 × 3.0 × 0.1 cm). Prior to exposure, the samples were polished on SiC paper in ethanol to 1000 mesh. They were then ultrasonically cleaned in ethanol, dried in air, and stored for a maximum of 24 h in a desiccator before the start of the exposure.

The experimental setup is illustrated in Fig. 1. It is made entirely of glass and Teflon. There are eight parallel corrosion chambers through which the gas is sequentially distributed, the whole gas flow passing through each chamber in turn for 15 s. The gas flow rate is 1000 ml/min in all

* Electrochemical Society Active Member.